

PETROGENESIS OF THE MOUNT STUART BATHOLITH
PLUTONIC EQUIVALENT OF THE HIGH-ALUMINA BASALT ASSOCIATION

by

Erik H. Erikson Jr.
Department of Geology
Eastern Washington State College
Cheney, Washington 99004

June 1, 1976

Abstract. The Mount Stuart batholith is a Late Cretaceous calc-alkaline pluton composed of intrusive phases ranging in composition from two-pyroxene gabbro to granite. This batholith appears to represent the plutonic counterpart of the high-alumina basalt association. Mineralogical, petrological and chronological characteristics are consistent with a model in which the intrusive series evolved from one batch of magnesian high-alumina basalt by successive crystal fractionation of ascending residual magma.

Computer modeling of this intrusive sequence provides a quantitative evaluation of the sequential change of magma composition. These calculations indicate that this intrusive suite is consanguineous, and that subtraction of early-formed crystals from the oldest magma is capable of reproducing the entire magma series with a remainder of 2-3% granitic liquid. Increasing potash discrepancies produced by the modeling may reflect the increasing effects of volatile transfer in progressively more hydrous and silicic melts.

Mass-balances between the amounts of cumulate and residual liquid compare favorably with the observed amounts of intermediate rocks exposed in the batholith, but not with the mafic rocks. Mafic cumulates must lie at depth. Mafic magmas probably fractionated by crystal settling, while quartz diorite and more granitic magmas underwent a process of inward crystallization producing gradationally zoned plutons ^{exposed} at present erosional levels.

INTRODUCTION

1. Geologic Setting

Calc-alkaline igneous intrusions in Washington State (USA) are exposed along the N-S axis of the Cascade Range and in north-central Washington (Fig. 1). The excellent exposures and rugged relief of the Cascade Range facilitates detailed studies of the structural and petrological character of these plutonic rocks.

The Mount Stuart batholith (1-3) and its outlying stocks are exposed over more than 500 km² in the central Cascades (Fig. 1). They have invaded the Chiwaukum Schist (1,6,7), a major pre-Cretaceous unit of the North Cascades, and a Jurassic ? mafic-ultramafic complex (1,8,9). All of these plutonic rocks are cut by several generations of mafic Tertiary dikes within the study area. The batholith and its host rocks comprise the Mount Stuart horst, a N-W trending early Tertiary structure (Fig. 1). This horst is bounded on the west by the Deception-Straight Creek fault (1,10,11), and on the east by the Leavenworth fault and Chiwaukum Graben (12). The southern margin of the horst is defined by arcuate zones of shearing within the serpentized mafic-ultramafic rocks.

2. Methods of Study

Nearly four complete field seasons were spent in the Mount Stuart area, 1970-73. Major element analyses were performed on 93 rocks from the batholith using atomic absorption techniques (13,14)¹. Analytical standards included seven Mount Stuart rocks independently analyzed by Dr. Norman Suhr (Pennsylvania State University) and U.S. Geological Survey standards⁽¹⁶⁾. All oxides determined are believed to be within 2-3% of the amount present. Each analyzed rock represents a homogenized composite of 4-5 kg, from which 0.25 g was used for fusion. The petrography of more than 400 thin sections was studied in detail, with point counts exceeding 1500 points (17). Additional chemical data incorporated

1 Complete analytical data is available on magnetic tape in file PETROS(15)

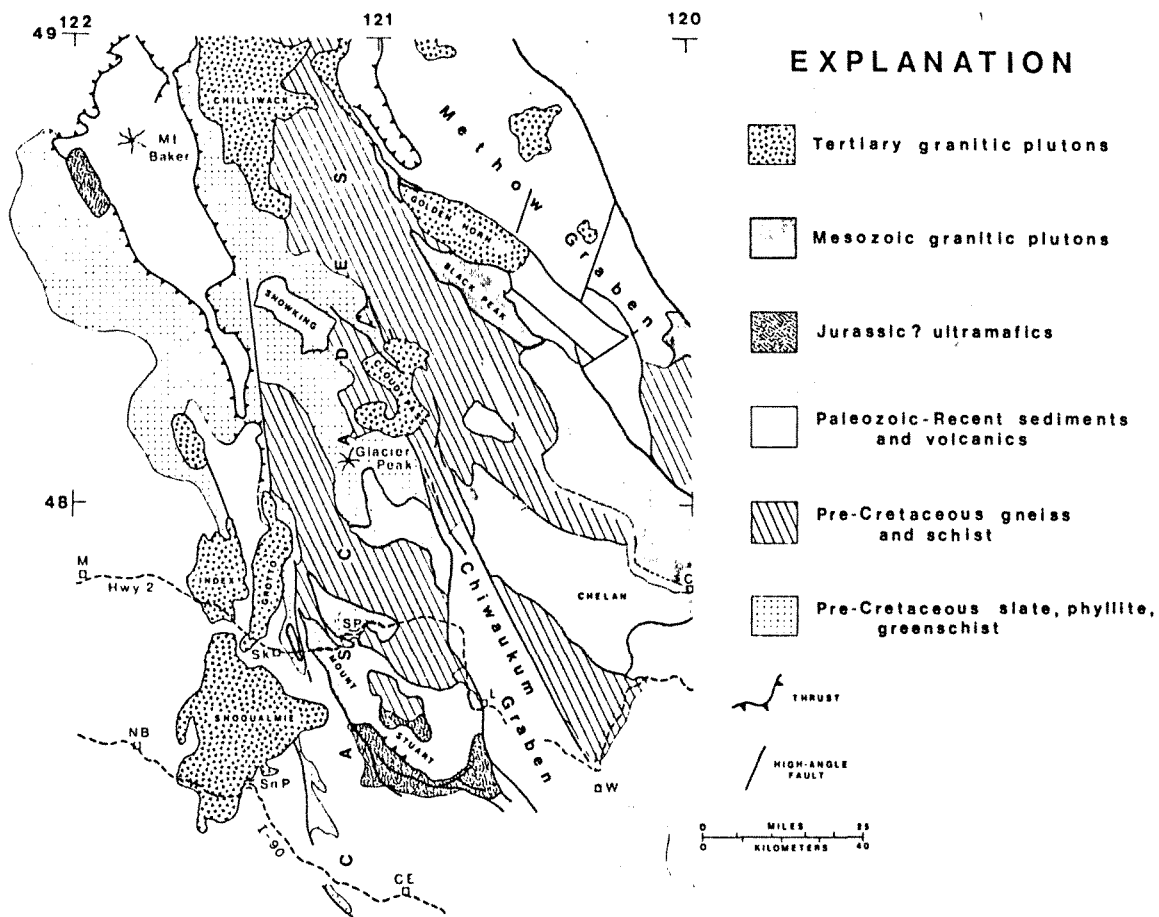


Fig.1. Generalized tectonic map of the northern Cascade Range, Washington (USA) and vicinity (4,5). C=Chelan, C E= Cle Elum, L= Leavenworth, M=Monroe, N B= North Bend, Sk= Skykomish, Sn P= Snoqualmie Pass, S P= Stevens Pass

in this study was gathered by Pongsapich(18), particularly his microprobe analyses of Mount Stuart minerals, and by Smith (3).

3. Acknowledgements

This study was made possible by grants from the National Geographic Society and the Geological Society of America. Their support is gratefully acknowledged. The cooperation and assistance of James Gualtieri (U.S. Geological Survey) played a significant role in the execution of the fieldwork. Capable field assistants included Alan Williams, Thomas Heffner, Chris Erikson, and Shawn Erikson. David Hoover assisted during the analytical stage of this study, and Pauline Masters prepared the computer programs. My thanks to Myron Best, Donald Hyndman, Felix Mutschler, James Snook, and Thomas L. Wright, who have significantly contributed to the preparation of this manuscript.

GENERAL CHARACTERISTICS OF THE MOUNT STUART BATHOLITH

K/A dating of coexisting biotite-hornblende pairs in the batholith and the out-lying Beckler Peak Stock ^{by (19)} has established a Late Cretaceous age of crystallization, 88 ± 2 m.y. (19). Additional exploratory dating has been done (19-22).

Evidence of igneous origin and multiple emplacement is inferred from:

1. Detailed mapping of systematic cross-cutting relationships; 2. The chemical and mineralogical homogeneity of intrusive phases comprising the batholith;
3. Flow-foliation which is parallel to intrusive contacts; and 4. Rock composition, mineralogy and texture (23). Intrusive units range in size from small plugs and dikes to plutons comprising large portions of the batholith (Fig. 2). The largest plutons exhibit compositional zoning. Cognate mafic inclusions, transformed by varying degrees of recrystallization, appear in all but the most leucocratic intrusives.

Fig. 2

Fig. 3

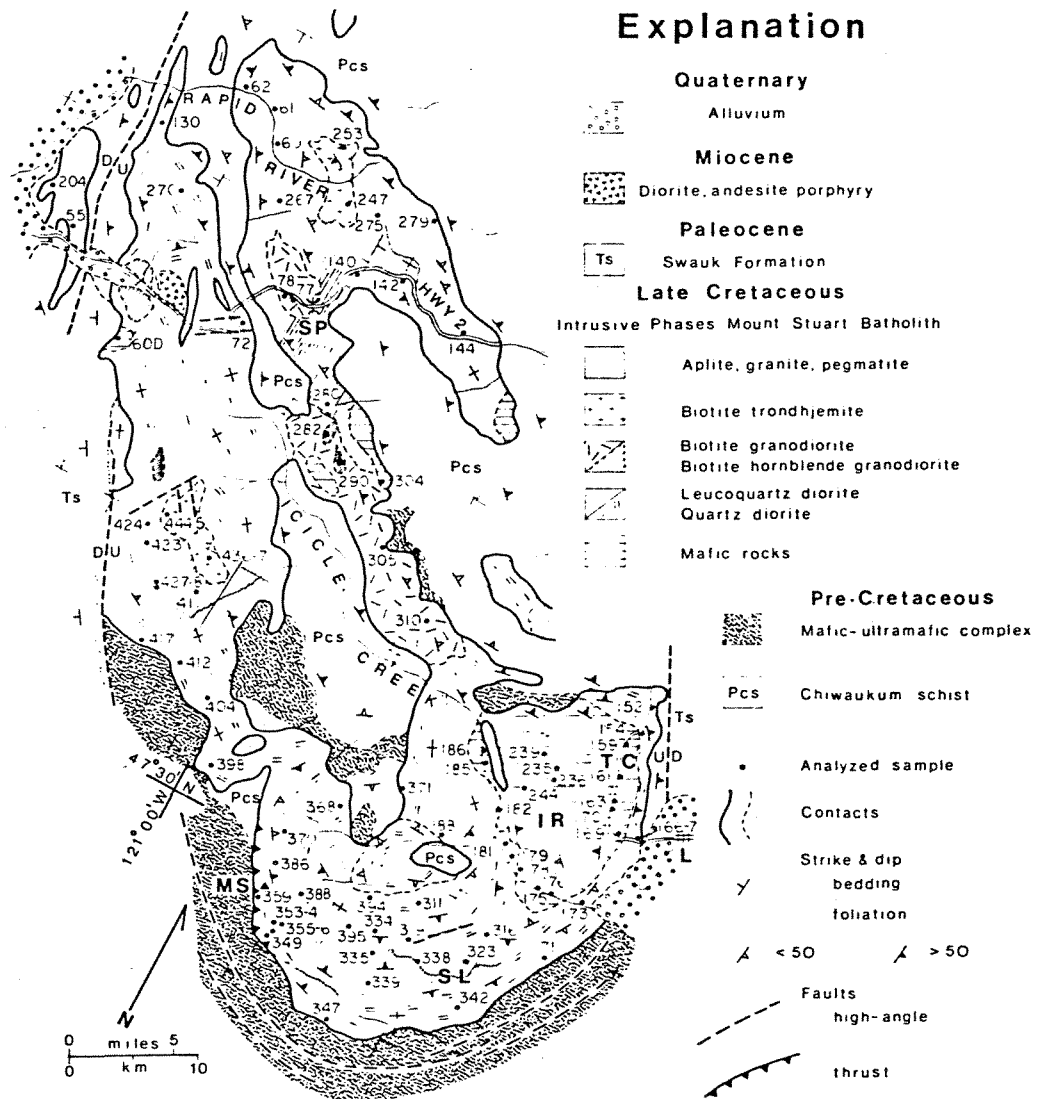


Fig. 2. The Mount Stuart batholith, central Cascade Mountains, Washington (USA). IR=Icicle Ridge, L=Leavenworth, MS=Mount Stuart, SL=Snow Lakes, SP=Stevens Pass, TC=Tumwater Canyon

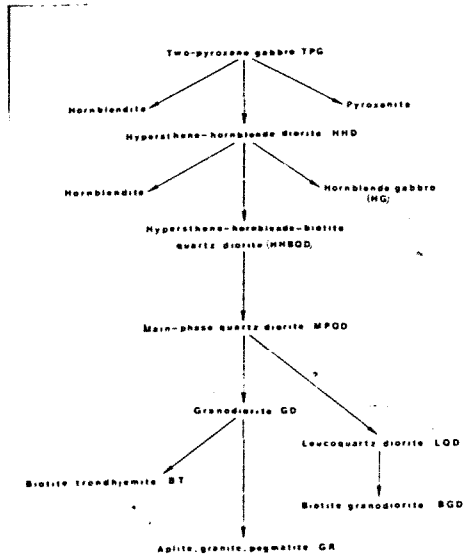


Fig. 3. The intrusive series and liquid line of descent of the Mount Stuart batholith

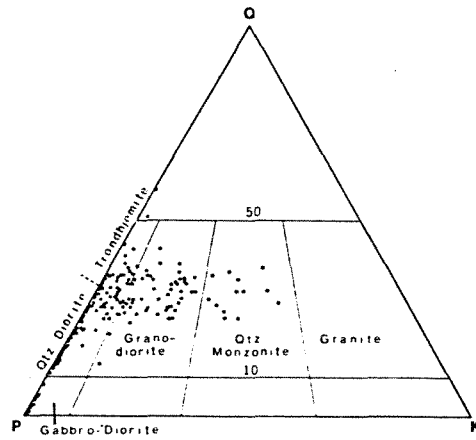


Fig. 4. Modes and nomenclature for Mount Stuart rocks. Q=quartz, P= plagioclase, K= K-feldspar

Most Mount Stuart rocks are foliated (Fig. 2). Foliation is largely the result of flow alignment of early-formed hornblende and plagioclase, rarely biotite. Prooclasis is locally developed adjacent to pluton margins. The overall structural fabric of individual plutons resembles gneiss domes.

Emplacement of the batholith as a whole was strongly controlled by the structures of the enclosing Chiwaukum Schist. This is suggested by the elongation of the batholith parallel to foliation and compositional layering within the schist. Emplacement began as mafic magmas invaded host rocks in the Icicle Ridge area. The upward movement of successively younger magmas, generated by fractionation at depth, stopped and dismembered older plutons. They rose as dike-like intrusives and semi-crystalline diapirs, progressively wedging apart the Chiwaukum Schist along its N-W trending structural grain. The motions of these magmas are defined by flow-foliation patterns within them. Smaller, more granitic stocks rose forcefully within their host plutons. Their hosts were, in some cases, incompletely crystalline as indicated by the stretching of cognate inclusions.

Pelitic schists and ultramafic contact rocks contain key assemblages for assessing the P-T conditions of contact metamorphism. Frost (8) suggests that T exceeded 725°C adjacent to quartz dioritic magmas. Coexisting sillimanite-andalusite-staurolite (7) indicate that pressures at the present erosional level were less than 4 kb (24-26).

INTRUSIVE SERIES OF THE MOUNT STUART BATHOLITH

Fig 4

1. Introduction

The intrusive series of the batholith ranges from two-pyroxene gabbro (norite) systematically through mineralogic varieties of gabbro, diorite, quartz diorite, granodiorite to trondhjemite and granite (Figs. 3,4). The proportions of these

rocks are given in Table 5, Column 3. Accumulate rocks include varieties of pyroxenite, hornblendite, and mafic gabbro, some containing olivine. The youngest phases include aplite and granite pegmatite. Hornblende- and plagioclase-enriched rocks occur at several stages within the intrusive suite and are spatially associated with their inferred parental rocks.

← Figs. 5, 6

Mafic minerals and plagioclase exhibit systematic changes in their composition, and their sequence of crystallization, throughout the rock series (Figs. 5, 6). Of particular interest is the early appearance of hornblende in the paragenetic sequence, an indicator of the minimum water content of their host magma.

2. Ultramafic and related rocks

A variety of medium-grained hornblende and pyroxene-rich rocks occur within the Icicle Ridge area (Fig. 2), although small bodies of these rocks are found locally throughout the batholith. All these rocks differ markedly in composition, mineralogy, and texture in comparison with the ultramafic wall rocks (1, 7-9, 18). Two groups of Mount Stuart ultramafic rocks have been identified. They differ primarily in their mineralogy, occurrence, and relative ages. All are poor in olivine.

← Table 1

The first group contains various proportions of brown hornblende, orthopyroxene, clinopyroxene, plagioclase, minor olivine, and opaques (Table 1). These rocks occur mainly as scattered inclusions in gabbro and diorite in the Icicle Ridge area (Fig. 2). Orthopyroxene and plagioclase in these inclusions are slightly more magnesian and calcic, respectively, compared to these same minerals in their host rocks. Accordingly, this group of ultramafic rocks is considered to have formed by segregation of early-formed minerals of their hosts, and are cumulates. No cumulate textures were recognized. Olivine (Fo 77) is found in sample 299 (Table 1), where it is surrounded and partially replaced by orthopyroxene (En 77). Most of these rocks

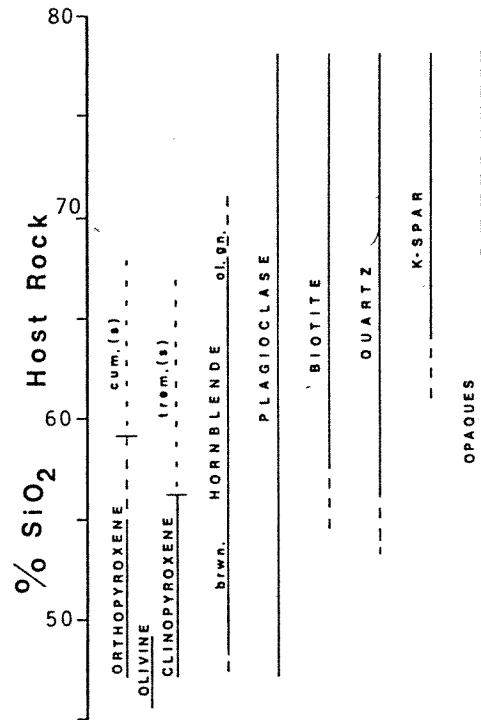


Fig. 5. Paragenetic sequence of the Mount Stuart intrusive series. Post-magmatic minerals include cummingtonite (cum) and tremolite (trem)

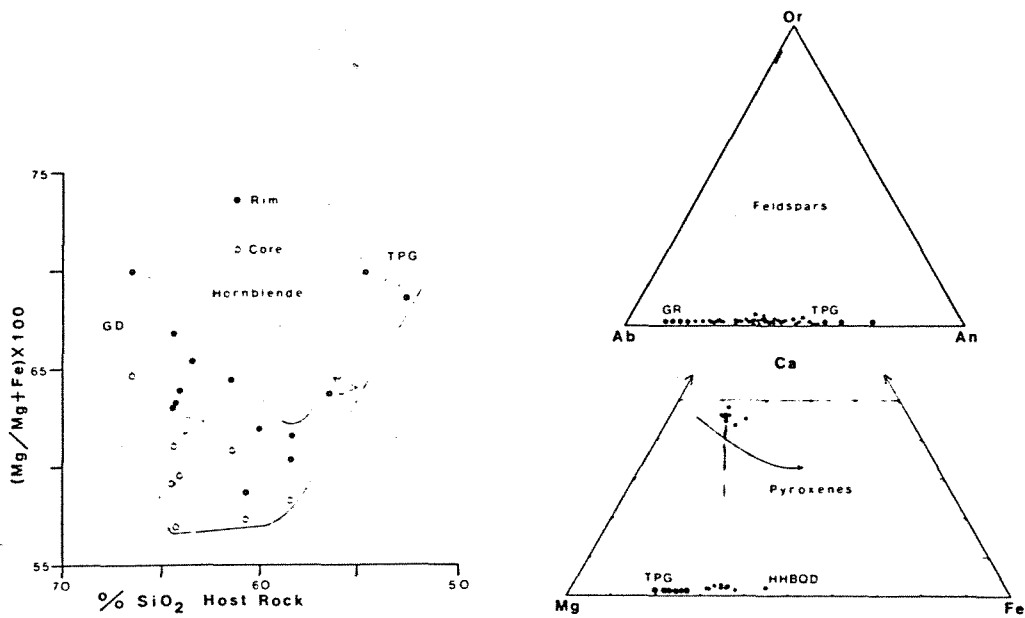


Fig. 6. Analyzed minerals from the Mount Stuart intrusive series. Symbols as Fig. 3. Large dots are optical determinations by author, small dots and hornblende compositions from Pongsapich(18)

Table 1. Representative ultramafic rocks of the Mount Stuart batholith

	Modes					
	Group 1					Group 2
	49B	161B	195A	244	299 ¹	182 ²
Olivine	-	-	-	-	2	-
Orthopyroxene	40	25	30	80	50	-
Clinopyroxene	50	-	5	-	15	-
Hornblende	10	75	40	20	10	90
Biotite	-	-	-	1	1	5
Plagioclase	-	-	20	-	24	3
Quartz	-	-	5	-	-	3
Opagues	tr	tr	tr	tr	tr	tr
Olivine ³	-	-	-	-	Fo 77	-
Orthopyroxene	En 77	En 80	En 74	En 73	En 77	-
Clinopyroxene N _z	1.703	-	1.700	-	1.704	-
Hornblende N _z	1.668	1.666	1.666	1.666	1.677	-
Plagioclase	-	-	An 50	-	An 65-48	An 35

1 Analyzed sample (loc. 299, Fig. 2)

2 Sample representative of Group 2

3 Refractive indices \pm 0.002, plagioclase by a-normal method if less than An 50, otherwise immersion oil techniques were used

have undergone various ^{amounts} of recrystallization, and possibly some primary olivine has recrystallized to orthopyroxene.

The second group is characterized by the predominance of olive-green hornblende and contains variable amounts of plagioclase, minor opaques and biotite. Sample 182 (Table 1) is representative of this group. These rocks occur as vein-like networks in quartz diorite and diorite, but their relative age compared to their host is inconclusive. Hornblende is optically similar to the hornblende of their hosts. These 'veins' may represent hornblende-enriched residual liquids. This origin is consistent with the paragenetic sequence (Fig. 3).

3. Mafic rocks

← Table 2

A large intrusive complex of mafic rocks underlies Icicle Ridge (Fig. 2). Smaller scattered bodies occur throughout the batholith, mostly along its contacts. Similar rocks have been identified in outlying stocks, such as at Big Jim Mountain, immediately north of Icicle Ridge (7). Mineralogic varieties of gabbro, diorite, and mafic quartz diorite have been recognized. These include, in order of decreasing age, two-pyroxene gabbro (TPG), hypersthene-hornblende diorite (HHD), hornblende gabbro, and hypersthene-hornblende-biotite quartz diorite (HHBQD) (Fig. 3, Table 2). The most notable characteristic of these rocks is their high magnesium content, manifested by the predominance of orthopyroxene over augite (about 3:1) and the presence of brown hornblende. These rocks typically contain secondary cummingtonite replacing hypersthene, and augite cores in some hornblende are replaced by tremolite-actinolite. Hornblende crystallizes relatively late in TPG, but forms at progressively earlier stages in succeeding younger mafic and intermediate rocks.

Table 2. Mean composition of major intrusive phases of the Mount Stuart batholith¹

	Two-pyroxene gabbro			Hypersthene-hornblende diorite			Hornblende gabbro ²		
		σ	SEM		σ	SEM		σ	SEM
SiO ₂	52.83	0.81	0.36	54.67	1.09	0.30	48.51	0.93	0.46
Al ₂ O ₃	16.69	0.91	0.41	16.73	1.09	0.30	17.48	1.93	0.96
Fe ₂ O ₃	8.39	0.40	0.18	7.20	0.77	0.21	8.59	1.58	0.79
MgO	9.74	1.72	0.77	7.64	1.49	0.41	9.46	3.09	1.54
CaO	8.15	0.14	0.06	7.88	0.47	0.13	10.09	1.13	0.56
Na ₂ O	3.24	0.27	0.12	3.52	0.28	0.08	2.70	0.54	0.27
K ₂ O	0.26	0.08	0.03	0.52	0.14	0.04	0.19	0.03	0.01
TiO ₂	0.83	0.08	0.03	0.79	0.10	0.03	1.07	0.05	0.02
MnO	0.16	0.00	0.00	0.13	0.02	0.00	0.16	0.05	0.02
Total	100.28			99.08			98.24		
Number of analyses		5		13			4		
Q		0.01		3.97			0.00		
C		0.00		0.00			0.00		
Or		1.54		3.12			1.15		
Ab		27.49		30.21			23.39		
An		30.33		28.72			35.36		
Di		6.53		7.06			9.95		
He		1.65		1.67			2.34		
En		21.31		16.03			10.18		
Fs		6.16		4.34			2.75		
Fo		0.00		0.00			6.54		
Fa		0.00		0.00			1.95		
Wo		0.00		0.00			0.00		
Mt		3.39		3.37			3.82		
Il		1.58		1.52			2.08		
Hm		0.00		0.00			0.00		
Ru		0.00		0.00			0.00		
Norm Plag		52.44		48.73			60.52		
D.I.		29.06		37.29			24.54		
C.I.		40.61		33.99			39.59		
Volcanic equivalent	High-alumina basalt K-poor series			High-alumina basalt average series			High-alumina basalt average series		

¹ Mean compositions based upon 172 analyses (the author, 3,18), total iron as Fe₂O₃, all values in weight percent except standard deviation (σ) and standard error of the mean (SEM), norm calculations and volcanic rock terminology after Irvine and Baragar (27). DI= Differentiation index, CI= Color index, Volume proportions appear in Table 5

² Position of hornblende gabbro in the intrusive series is inconclusive

Table 2 Cont.

Hypersthene-hornblende- biotite quartz diorite			Main-phase Quartz diorite			Rapid River Leucoquartz diorite		
	σ	SEM		σ	SEM		σ	SEM
56.89	1.67	0.33	62.29	2.69	0.32	68.49	1.93	0.64
16.66	1.90	0.38	16.43	0.66	0.08	15.90	0.38	0.12
6.28	1.60	0.32	4.58	0.89	0.11	3.37	0.86	0.29
6.15	1.82	0.36	3.71	1.15	0.14	1.63	0.75	0.25
6.96	0.67	0.13	5.26	0.80	0.10	4.20	0.46	0.15
3.73	0.52	0.10	3.98	0.20	0.02	3.82	0.59	0.19
0.97	0.38	0.08	1.63	0.30	0.04	1.77	0.41	0.14
0.85	0.17	0.03	0.66	0.14	0.02	0.38	0.14	0.05
0.12	0.03	0.01	0.08	0.02	0.00	0.07	0.01	0.00
98.61			98.62			99.62		
25			69			9		
7.89			16.64			28.02		
0.00			0.00			0.06		
5.84			9.80			10.52		
32.13			34.23			32.49		
26.32			22.52			20.94		
5.89			2.32			0.00		
1.13			0.34			0.00		
12.86			8.08			4.08		
2.83			1.11			0.41		
0.00			0.00			0.00		
0.00			0.00			0.00		
0.00			0.00			0.00		
3.47			3.18			2.74		
1.64			1.27			0.72		
0.00			0.00			0.00		
0.00			0.00			0.00		
45.03			39.70			39.20		
45.35			60.67			71.03		
27.83			16.82			7.96		
High-alumina basalt average series			High-alumina andesite average series			Tholeiitic andesite average series		

Table 2 Cont.

Granodiorite			Stevens Pass Biotite granodiorite			Biotite trondhjemite		
	σ	SEM		σ	SEM		σ	SEM
66.62	2.20	0.47	74.77	0.23	0.13	72.57	0.92	0.46
15.39	0.50	0.11	13.58	0.30	0.17	15.05	1.18	0.59
3.57	0.38	0.08	1.76	0.24	0.14	1.39	0.50	0.25
2.39	0.64	0.14	0.65	0.12	0.07	0.45	0.19	0.09
4.09	0.59	0.12	1.95	0.13	0.07	2.75	1.03	0.51
3.92	0.23	0.05	3.94	0.39	0.22	5.07	0.57	0.28
2.29	0.31	0.07	3.07	0.34	0.20	2.22	0.50	0.25
0.52	0.13	0.03	0.17	0.06	0.03	0.15	0.13	0.06
0.09	0.14	0.03	0.05	0.01	0.00	0.04	0.01	0.00
99.39			99.93			99.70		
22			3			4		
23.09			34.97			28.51		
0.00			0.23			0.00		
13.65			18.17			13.17		
33.42			33.36			43.03		
19.14			9.68			11.78		
0.99			0.00			1.48		
0.03			0.00			0.00		
5.54			1.62			0.44		
0.19			0.00			0.00		
0.00			0.00			0.00		
0.00			0.00			0.00		
0.00			0.00			0.00		
2.95			0.00			0.00		
0.99			0.28			0.08		
0.00			1.67			1.39		
0.00			0.02			0.10		
36.40			22.50			21.50		
70.16			86.50			84.71		
10.69			3.57			3.40		
High-alumina andesite average series			Dacite average series			Dacite K-poor series		

4/4

Table 2 Cont.

Aplite, quartz monzonite,
granite

	σ	SEM
76.24	0.97	0.29
13.30	0.51	0.15
0.67	0.29	0.09
0.10	0.07	0.01
1.17	0.42	0.13
3.80	0.51	0.15
4.21	0.90	0.27
0.14	0.14	0.04
0.03	0.01	0.00
<hr/>		
99.65		

11

35.47
0.36
24.99
32.26
5.82
0.00
0.00
0.25
0.00
0.00
0.00
0.00
0.00
0.00
0.06
0.67
0.11

15.30
92.72
0.99

Rhyolite
K-poor series

Hypersthene-hornblende diorite (HHD) is the most abundant rock in the mafic complex. The younger hypersthene-hornblende-biotite quartz diorite (HHBQD) forms a discontinuous shell surrounding the main-phase quartz diorite (MPQD). No field or chemical evidence exists for extensive assimilation of these older mafic rocks by younger intrusive phases, although they have locally been intensely dismembered. The position of hornblende gabbro within the intrusive sequence is inconclusive. It is characterized by the presence of brown hornblende and contains numerous hornblende-rich clots.

4. Quartz diorite, granodiorite, trondhjemite

Foliated quartz diorite and granodiorite comprise 85% of the batholith (Fig. 2, Table 5). Distinctive mineralogical, textural, and compositional varieties of these rocks have been distinguished. Two of the largest plutons, the main-phase quartz diorite and the Rapid River leucoquartz diorite, exhibit gradational compositional zoning. More mafic and calcic quartz-dioritic margins grade inward into varieties of granodiorite, and locally leucogranodiorite (Fig. 2). However, distinct plutons of granodiorite and leucogranodiorite with intrusive contacts also exist. The mineralogical and compositional variations of these rocks correspond to different ratios of hornblende to biotite, potassium feldspar to plagioclase, and variations in their quartz content (Fig. 4, Table 2). Pongsapich (18) recognized that Mg/Mg+Fe zoning in hornblende in quartz diorite and granodiorite resulted from the simultaneous crystallization of biotite with hornblende rims. Mg/Fe partitioning between the two minerals caused the hornblende rims to become progressively more magnesian (Fig. 6). Hornblende is noticeably not zoned in more mafic rocks, where biotite is absent or forms late.

^
Andesine leucoquartz diorite is an unusual rock found as dikes in MPQD in the Icicle Creek valley and to the south. Apparently, it is a type of

mafic depleted residual liquid of fractionated MPQD magma.

Biotite trondhjemite occurs as stocks and dikes on French Ridge (loc. 444, Fig. 2) and northwest of Lake Valhalla (loc. 247). These stocks have numerous apophyses extending outward from their margins, which are in turn cut by aplite swarms. Typically, biotite is the sole mafic mineral.

5. Aplite, granite, pegmatite

This group of rocks forms sill-like sheets, dikes, en echelon fracture fillings and small plugs. They most commonly are associated with granodioritic rocks but also may be found in quartz diorite. Several episodes of aplite injection, with very minor differences in bulk composition and mineralogy, can be recognized. Mirolitic cavities are present in some granites and pegmatites indicating the presence of a late fluid phase. All granitic rocks consist of proportions of quartz, sodic oligoclase, micropertthitic orthoclase with an intermediate structural state, chloritized biotite and occasional secondary muscovite, schorl, rose quartz, epidote, spessartite, pyrite and chalcopyrite. Crude mineralogic zoning appears in some pegmatite dikes.

PETROCHEMICAL RELATIONSHIPS

✓ Figs 7,8

Chemical variations of the Mount Stuart intrusive series (Figs. 7,8) correspond to trends typical of calc-alkaline magma suites with two prominent exceptions. The soda/potash ratio maintains relatively high levels throughout the series in comparison with other magma suites. This is reflected in the typically higher ratio of sodic plagioclase to potash feldspar, and is related to initial low levels of potash in the inferred parent magma. The sum of the alkali oxides is similar to other batholithic suites. The alkali-lime index was determined to be $62 \pm 1\% \text{ SiO}_2$, intermediate between the Idaho and Sierra Nevada suites, 60 and 60.5% SiO_2 , and the Snoqualmie and Southern California suites, both

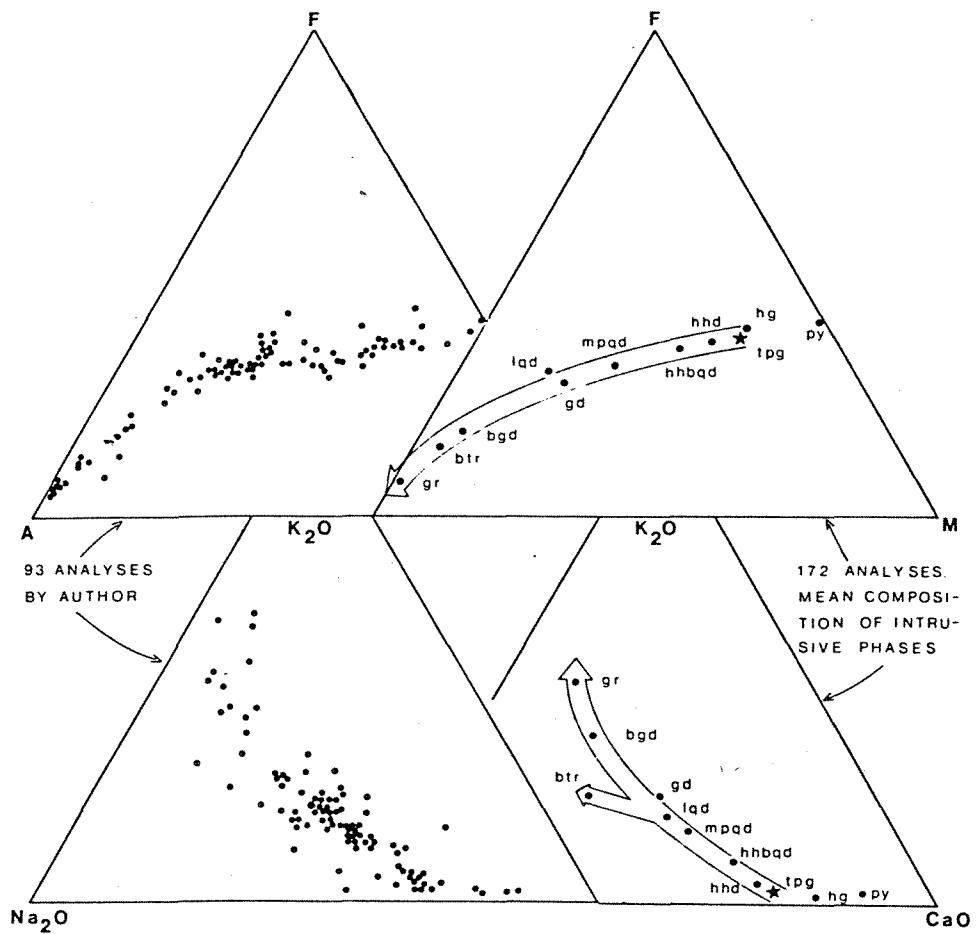


Fig. 7. Chemical trends and liquid line of descent of the Mount Stuart intrusive series. Symbols as in Fig. 3. A= $Na_2O + K_2O$, F=total iron as FeO , M= MgO . Mean compositions from Table 2

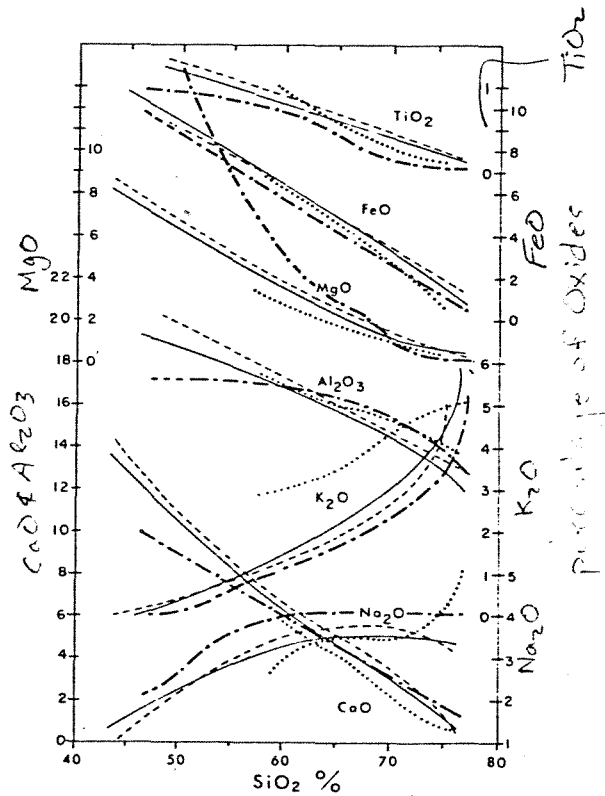


Fig. 8. Comparison of oxide variations of the Mount Stuart batholith (bold dash-dot) with those of the Sierra Nevada batholith (dotted), the Southern California batholith (dashed), and the Snoqualmie batholith (solid) (28-30). Total iron as FeO

63.5% SiO₂ (28-30).

← Fig. 9

The second unusual characteristic is the high magnesium level of the mafic and intermediate rocks of the Mount Stuart series (Figs. 8,9). These rocks are more magnesian than corresponding rocks of other intrusive and volcanic suites.

EVOLUTION OF THE MOUNT STUART MAGMA SUITE

1. Introduction

All mineralogical and petrological features of the Mount Stuart intrusive series are consistent with the hypothesis that it has evolved from a single batch of high-alumina basalt by successive fractional crystallization of ascending residual magma. The main arguments for this model include the following:

1. Systematic changes in the composition of minerals and their host rocks throughout the intrusive series;
2. Intrusive phases become increasingly more granitic with decreasing age;
3. Computer simulation of this fractionation process provides quantitative evidence that removal of early-formed crystals from the oldest magma can form the entire rock association.

One serious discrepancy mitigating against the model is the lack of sufficient mafic cumulate within the batholith. The cumulate formed during the generation of HHD, HHBQD, and MPQD is missing and must lie at depth, if it exists at all. However, appropriate amounts of more granitic rocks which satisfy mass-balance requirements appear in the batholith. All these points are discussed in more detail below.

2. Proposed Parental Magma

The relative abundance of intermediate rocks in batholiths and the great abundance of corresponding andesitic volcanic rocks has been used to suggest that

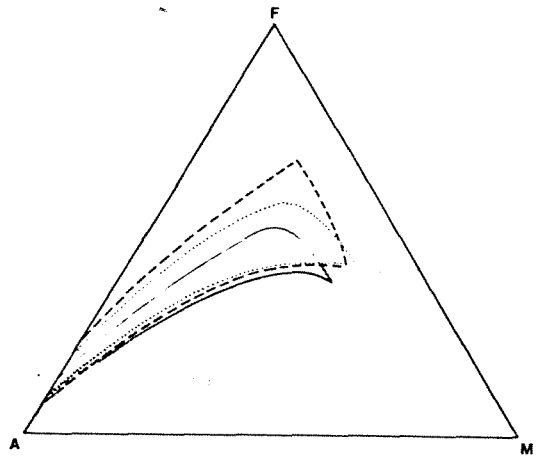


Fig. 9. Comparison of chemical variations of the Mount Stuart batholith (shaded, 172 analyses) with the Japanese volcanic arc (dashed, 1102 analyses), Cascade Tertiary plutonic-volcanic rocks (dotted, 937 analyses) and the Sierra Nevada batholith (solid, 266 analyses), data from Mutschler and others(15)

andesites are the parent magmas for calc-alkaline batholiths. This may be true for some batholiths; however, volume relationships alone are not satisfactory criteria for the choice of parental magmas. Nockolds and Allen (31) and Bowen (32) chose parental magmas based upon chemical trends of ^{their} rock associations. More importantly, there must be consistency between all pertinent data; field relationships demonstrating the intrusive sequence, chemical trends of minerals and their host rocks, and mass-balance relationships.

The oldest intrusive phase identified in the batholith is believed to be the parental magma for this intrusive suite. As it turns out, even the younger HHD could be the parent magma, but the older TPG is favored. Two-pyroxene gabbro (TPG) has a fine-grained sub-porphyrific texture characteristic of chilled magma. TPG occurs as inclusions in younger HHD and HHBQD. Although fractionation of TPG occurred at depth, the inclusions represent dismembered apophyses and/or fragments of the crystalline wall¹ of the TPG fractionation chamber. Mafic minerals and plagioclase of succeeding younger intrusives define compositional trends away from corresponding TPG minerals (Figs. 5,6). Younger hornblendes and pyroxenes exhibit decreasing $MgO/MgO+FeO$ and plagioclase shows decreasing $CaO/CaO+Na_2O$. Furthermore, subtraction of olivine (Fo 77), hypersthene (En 77), augite (Di 76), sodic labradorite, and opaques, in reasonable amounts from TPG can produce all the younger rocks found in the batholith. These minerals were identified as early-formed minerals in thin section. Modes of representative cumulates formed by computer modeling appear in Table 6. The olivine-bearing rocks formed as cumulates during fractionation of TPG have not been seen in the batholith. The olivine content of ^{exposed} gabbroic or ultramafic rocks rarely exceeds several percent, but some olivine may have been recrystallized to hypersthene since most of these ^{rocks} have undergone variable degrees of recrystallization. Cumulates (Table 6) are gabbroic, but not ultramafic. ^{as computed by Method 1}

TPG corresponds to the composition of high-alumina basalt as defined by Irvine and Baragar (27), Table 2. Their widespread distribution and associated rocks have been documented in the circum-Pacific region, particularly in Japan, and in the High Cascades of Washington and Oregon (33-37). The Mount Stuart magma series, although relatively more magnesian, parallels the fractionation trends observed from high-alumina basalt associations of those regions (Fig. 9). No volcanic equivalents of the Mount Stuart series are preserved, but presumably shallow to intermediate depth plutons like the Mount Stuart erupted lava onto the surface.

3. Computer Modeling of Fractionation

The proposed fractionation process was evaluated by means of a linear-programming least-squares computer program designed by Wright and Doherty (38). Two methods of computation were used. Both methods used the following relationship, but each applies it differently:

$$(1) \quad \begin{array}{l} \text{Parent Magma} \\ \text{(older intrusive phase)} \end{array} = \begin{array}{l} \text{Liquidus Crystals} \\ \text{(of parent)} \end{array} + \begin{array}{l} \text{Residual Liquid} \\ \text{(younger intrusive phase)} \end{array}$$

For the first method, Equation (1) was applied step-wise along the intrusive series (Fig. 3), whereby, the older phase was substituted for the parent at each step, and the next younger phase was substituted for the daughter residual liquid. By contrast, Method 2 utilized TPG as the parent for all succeeding phases, and it calculated directly the amount of each phase produced by the subtraction of early-formed crystals from TPG. Method 1 corresponds more closely to the proposed fractionation process, whereas Method 2 is merely an additional test of the feasibility of the process.

During Method 1 calculations each 'parental' rock along the series is treated as though each ^{rock} is a liquid. Essentially, the program calculates the amount and composition of the liquidus minerals, and the amount of the residual liquid

Table 3

Table 3. Results of Method 1: Step-wise fractionation of parental basalt (TPG)*

	Parent	Daughter	Minerals	Fo 90	Fo 77	Cpx	Opx	Ho	Biot
1.	TPG	HHD	W-245	5.38	—	4.87	14.55	—	—
2.	"	"	W-255	4.54	—	6.85	16.64	—	—
3.	"	"	W-387	—	—	6.53	14.65	—	—
4.	"	"	W-245	—	9.75	6.12	6.90	—	—
5.	"	"	W-255	—	6.75	6.35	14.22	—	—
6.	HHD(W-53A)	HHBOD(MS-159)	W-53A	—	—	1.81	4.85	—	—
7.	"	HHBQD(MS-179)	W-53A	—	—	2.54	—	—	—
8.	HHD	HHBQD	W-53A	2.23	—	5.99	13.02	—	—
9.	"	"	W-53A	—	—	6.42	17.52	—	—
10.	HHBQD(W-44A)	MPQD(W-675)	W-44A	—	—	6.13	14.10	—	—
11.	"	MPQD	W-44A	—	—	4.77	11.73	—	—
12.	MPQD	GD(W-610)	W-304	—	—	—	—	7.82	2.04
13.	MPQD(W-304)	GD(W-610)	W-304	—	—	—	—	4.94	0.51
14.	MPQD	GD	W-274	—	—	—	—	10.68	2.81
15.	"	"	W-675	—	—	—	—	11.70	1.95
16.	MPQD(W-304)	GD	W-304	—	—	—	—	7.54	1.30
17.	MPQD(W-675)	LOD	W-675	—	—	—	—	3.71	5.03
18.	MPQD	LQD	W-274	—	—	—	—	11.26	6.11
19.	"	"	W-274	—	—	—	—	16.46	—
20.	GD(W-413)	BT	W-413	—	—	—	—	13.76	8.06
21.	"	"	W-413	—	—	—	—	12.44	8.66
22.	GD(W-610)	GR	W-610	—	—	—	—	14.48	3.82
23.	"	"	W-610	—	—	—	—	13.69	3.03
24.	GD(W-413)	GR	W-413	—	—	—	—	16.93	3.73

* Fractionation computed along the liquid line of descent in Fig. 3. Parent= mean composition of intrusive units from Table 2, except where sample number indicates a specific rock composition used. Daughter= mean composition of intrusive units from Table 2, except where a specific rock is identified. Liquid= amount of daughter formed by subtraction of minerals from parent. Symbols of parent and daughter as in Fig. 3. Minerals= early-formed phases identified in the rocks specified. Olivine: Fo 90 is used for purposes of comparison, Fo 77 actually found in sample 299. Orthopyroxene (Opx), clinopyroxene (Cpx), hornblende (Ho), biotite (Biot), magnetite (Mt), ilmenite (Ilm), plagioclase (Plag) and derived composition of plagioclase (%An). Mineral analyses from Pongsapich (18) and optical determinations by the author, Table 1. Biotite, magnetite, and ilmenite from other sources (39-41). 'Largest residual' is the greatest difference between the computed and actual composition of the parent. All values in weight percent

Table 3. Continued

Mt	Ilm	Plag	% An	"Liquid"	Largest Residual
0.68	1.03	33.60	44.8	39.91	+0.01 K ₂ O
1.00	1.26	42.58	50.5	26.15	-0.04 MnO
1.48	0.98	33.92	52.4	42.47	+0.11 K ₂ O
1.22	1.01	36.36	46.3	46.27	+0.32 Na ₂ O
0.65	1.19	39.60	51.2	31.30	-0.05 MnO
1.58	0.59	26.12	40.3	65.04	+0.20 K ₂ O
2.38	0.64	26.24	36.5	68.23	+0.23 SiO ₂
—	0.75	31.51	49.2	46.52	+0.02 K ₂ O
—	0.35	34.14	50.3	41.59	+0.35 MgO
—	1.14	47.72	42.8	30.93	-0.17 K ₂ O
0.21	1.06	42.40	42.8	39.86	-0.10 K ₂ O
0.52	—	18.03	31.1	71.61	+0.23 K ₂ O
0.30	—	9.78	26.5	84.50	+0.24 K ₂ O
0.06	0.29	20.30	34.1	65.90	+0.21 K ₂ O
—	—	18.65	34.0	67.71	-0.28 MgO
0.77	—	17.46	31.74	72.96	+0.19 K ₂ O
—	0.12	15.13	38.9	76.04	+0.02 K ₂ O
—	0.10	22.90	38.0	59.64	-0.23 MgO
—	—	22.04	27.6	61.52	+1.00 SiO ₂
—	—	20.55	40.46	57.65	+0.58 Na ₂ O
—	—	14.65	34.6	64.28	-0.25 MgO
—	—	33.75	36.4	47.19	+0.31 K ₂ O
0.80	0.66	33.66	37.5	48.19	+0.29 K ₂ O
1.00	—	32.49	38.8	45.87	+0.37 K ₂ O

(in the form of the next younger intrusive phase) which ~~are~~^{is} needed to produce the composition of the parent (the older intrusive phase). Early-formed minerals were identified in thin section, and their compositions were determined by microprobe analysis (18). Actual biotite and opaque minerals were not analyzed, but suitable compositions were chosen from other plutonic rocks (39-41). Rock analyses used were generally the mean compositions of intrusive units from Table 2, but in some instances single rock analyses were substituted for mean compositions. Differences between the computed 'parent' composition and the actual values are termed residuals. Residuals were compared with the standard deviation (σ) and the standard error of the mean (SEM) of each oxide in order to evaluate the fit. Both core and rim compositions of plagioclase and hornblende were entered, where these two minerals appeared as liquidus phases. The proper mixture of end-members were blended by the program to provide optimum solutions.

A summary of the results of Method 1 calculations appears in Table 3. Samples of typical cumulates produced at each stage of fractionation appear in Table 6. Judging from the small residuals, it is possible to derive the entire rock series from the initial TPG by subtraction of these minerals actually appearing in these rocks. Table 5 (Cols. 4-8) summarizes the amounts of residual liquids formed at each stage of the proposed fractionation process. Considering the mass-balances of basalt fractionation, reasonable amounts of residual granite liquid are produced, about 2-3% of the TPG. Granite, in the form of aplite, pegmatite, etc., comprises about this amount of the exposed batholith. For the earliest-
 mafic
 formed residual liquids, there is little correspondence between the amounts calculated at each step of differentiation and the amounts exposed in the batholith. This relationship is to be expected, since differentiation of mafic liquids took place at deeper levels, forming cumulates ^{and} _^ thereby changing their original compositions and amounts by the time they reached present erosional levels in the batholith.

Throughout the fractionation calculated by Method 1, potash exhibits

increasingly larger residuals (Table 3). In most cases this means that the liquid is enriched, or alternatively, the parent is depleted in potash. This same effect could be caused by inaccurate potash concentrations in plagioclase. If real, the K_2O residuals imply that this increase throughout the series was not altogether the result of simple crystal fractionation, but instead, the increasing effects of volatile transport (42) ⁱⁿ increasingly more hydrous and silicic melts.

A dozen rocks from other batholithic suites were substituted into the calculations for Mount Stuart rocks in order to test whether or not any rock of suitable composition would provide reasonable solutions. Some rocks from other suites did provide solutions within the SEM limits, but the majority of them required the use of mineral types, compositions, and proportions which were not compatible with the chemical characteristics of the Mount Stuart series. For instance, rim compositions rather than core compositions of hornblende and/or plagioclase ^{were} required (i.e. not early-formed minerals), or unreasonable proportions of minerals were required.

One obvious objection to Method 1 is that mean compositions of intrusive units are used as though each was an actual liquid. It is clear that each rock contains minerals which were in 'equilibrium' with the liquid from which they crystallized. The fractionation process assumes that some of the liquid escaped periodically and evolved separately. There is no sure way to determine how closely the rocks approach the composition of the liquid from which they crystallized. ^{However,} ^{quench} textures possibly provide the best clue, and on this basis, the TPG and the much younger aplite (GR) closely approximate the composition of their liquids.

Method 2 attempts to model an even more simplified fractionation process. Basically, it resolves the same question as before: Can the subtraction of liquidus minerals from TPG form directly, rather than in a step-wise fashion,

Table 4. Results of Method 2: Direct fractionation from basaltic parent (TPG)*

Intrusive phase	Fo 90	Fo 77	Cpx	Opx	Mt	Ilm	Plag	% An	"Liquid"	Largest residual
HHD	5.54	—	6.83	16.64	1.0	1.26	42.58	50.5	26.15	-0.04 MnO
HHD		6.75	6.35	14.22	0.65	1.19	39.60	51.2	31.27	0.00
HFBQD	6.15	—	8.40	19.23	1.16	1.44	49.72	50.6	13.93	-0.05 MnO
HFBQD	—	7.32	8.36	18.37	0.73	1.45	49.94	50.7	13.87	+0.01 K ₂ O
MPQD	6.78	—	9.27	19.81	1.35	1.58	53.43	50.6	7.82	-0.05 MnO
MPQD	—	3.07	9.22	18.87	0.86	1.59	53.67	50.6	7.75	+0.06 MnO
LQD	8.03	—	9.63	17.83	1.71	1.64	54.04	50.3	7.16	-0.06 MnO
LQD	—	9.50	9.56	16.81	1.13	1.65	54.35	50.5	7.03	+0.01 K ₂ O
GD	6.36	—	9.46	21.29	1.22	1.64	55.9	50.1	4.20	-0.05 MnO
GD	—	7.57	9.41	20.40	0.77	1.65	56.1	50.2	4.17	-0.05 MnO
SPGD	7.14	—	9.61	19.99	1.48	1.68	56.17	50.3	3.97	-0.05 MnO
SPGD	—	8.51	9.56	18.96	0.98	1.68	56.39	50.4	3.95	-0.06 MnO
BT	7.41	—	9.49	19.54	1.56	1.68	54.93	51.0	5.44	-0.06 MnO
BT	—	8.80	9.43	18.53	1.03	1.69	55.19	51.2	5.37	-0.06 MnO
GR	6.57	—	9.59	21.22	1.32	1.68	56.77	50.1	2.87	-0.05 MnO
GR	—	7.83	9.54	20.29	0.86	1.68	56.97	50.2	2.86	-0.05 MnO

* 'Intrusive phase' represents the residual 'liquid' whose computed amount is shown as 'liquid', all amounts in weight percent, SPGD= Stevens Pass granodiorite, other symbols as Table 3

Table 4

the different intrusive phases of the batholith? Method 2 is a one-step linear subtraction model which uses the same TPG parent to derive all subsequent units (Table 2), except for hornblende gabbro, which is of inconclusive age. Table 4 summarizes the results of these calculations. Excellent matches are obtained. Judging from the very small residuals, the amounts of residual liquids compare favorably with those of Method 1 (Table 5, Col. 5). Potash discrepancies do not appear in this method because of its linear approach. Again, a few percent of granite liquid is produced, consistent with Method 1 and field relations.

4. Mass-balance Implications

Table 5

Tables 5 and 6 summarize the data pertinent to mass-balance and petrogenesis for this magma series. According to Table 5, when crystallization of TPG is 63% complete (Col. 6) (the amount of accumulate formed), the remaining 37% is residual liquid with a composition of HHD. Subsequent fractionation of HHD liquid forms HHBQD when 45% of it has crystallized, forming accumulate, and the remaining 55% of the amount of HHD liquid remains, with the composition of HHBQD. At this point 20% of the total amount of parent TPG magma is still liquid (Col. 5), and so forth.

Table 6

Major volume discrepancies can be observed from Table 5, particularly for mafic magmas and their accumulates. Although fractionation is chemically feasible, based upon the calculations, mass-balance relations at the mafic end of the magma series presents serious discrepancies between observed and predicted amounts of rocks. By contrast, mass-balances among the intermediate and more granitic rocks agree quite well. As is typical of other batholiths, intermediate and more granitic rocks comprise 85 to 90 % of the Mount Stuart batholith (Col. 3). Mafic cumulate which must have been subtracted from TPG to form these intermediate to granitic rocks comprise only a minor fraction of

Table 5. Mass-balance relationships *

1	2	3	4	5	6	7	8
Intrusive Phase-	Mean Density	% Volume Exposed	Ave. Wt% Residual Liquid	% Res. Liquid Remaining	Ave. Wt% Crystal Cumulate	Ratio Liq./Cum.	Amt. TPG Needed
TPG	2.95	1-2	100	100	-	-	-
HHD	2.89	5	37	37	63	0.5	3X
HHBQD	2.81	5	55	20	45	1	5X
MPQD	2.74	50	36	7	64	0.5	14X
LQD	2.70	22	66	5	34	2	20X
GD	2.71	13	73	5	27	3	20X
GR	2.63	1	61	3	39	1.5	50X
BT	2.60	2	61	2	39	1.5	33X

* Symbols as in Fig. 3. Exposed volumes of rock units within the batholith are accurate to about $\pm 10\%$ of the amounts present, as estimated from Fig. 2. Mean densities determined from a minimum of five typical rocks from each unit. All additional data was derived from Method 1 calculations, Table 3 as determined along the liquid line of descent, Fig. 3. 'Residual liquids' are those liquids having a composition identical to the intrusive phase at the stage of fractionation identified. Col. 5 is the amount of original volume of TPG liquid remaining. Col. 8 is the amount of 'parental' TPG needed to form the residual liquid at each stage of fractionation

Table 6. Modes of representative cumulates formed by computed fractionation, Method 1*

Line	4	5	6	9	10	12	14	17	22
Parent	TPG	TPG	HHD	HHD	HHBQD	MPQD	MPQD	MPQG	GD
Residual Liquid	HHD	HHD	HHBQD	HHBQD	MPQD	GD	GD	LQD	GR
Plag % An	59 46	57 51	75 40	58 50	69 43	63 31	59 34	63 39	65 36
Fo 77	16	10	-	-	-	-	-	-	-
Cpx	10	9	5	11	9	-	-	-	-
Opx	11	21	14	30	20	-	-	-	-
Ho	-	-	-	-	-	27	31	15	28
Biot	-	-	-	-	-	7	8	21	7
Mt	2	1	4	-	-	2	tr	-	-
Ilm	<u>2</u>	<u>2</u>	<u>2</u>	<u>1</u>	<u>2</u>	<u>-</u>	<u>1</u>	<u>tr</u>	<u>-</u>
TOTAL	100	100	100	100	100	99	99	99	100

* Modes recalculated from Table 3, lines refer to assemblage of early-formed minerals numbered horizontally in Table 3. All symbols as in Table 3 and Fig. 3

the batholith. Magma energy budgets do not permit complete digestion of these refractory materials. From Table 5, (Col. 6) 63% of TPG must form mafic cumulate, and 45% of the HHD liquid produces cumulate as HHBQD is formed. The total amount of this cumulate produced by these two stages of fractionation is considerable: 80% of the total amount of TPG. This amount of TPG can be judged from the exposed amount of MPOD which requires 14 times as much TPG (Col. 8). ^{The total amount of} cumulate produced by the ^{time} HHBQD ^{is formed} is then 80% of 14 X 250 km². These mafic cumulates are olivine gabbro and two-pyroxene gabbro (Table 6), not ultramafic rocks. No olivine gabbro of this type appears in the batholith. Exposed cumulate-type rocks are poorer in ^{both} plagioclase and olivine (Table 1).

Assuming fractionation produced this magma series, cumulates produced by the early mafic magmas must lie at depth, a seemingly fortuitous circumstance. However, basaltic magmas (TPG, HHD, HHBQD) are fluid enough to permit early-formed crystals to sink. Also, fractionation of these magmas took place at greater depths than present erosional levels. The slightly greater densities of mafic cumulates, and a position near the bottom of the magma chamber, will inhibit their rise during the ascent of their residual liquids. Pertinent gravity data collected by Dr. Danes (University of Puget Sound) has not been studied to see if cumulates can be recognized beneath the batholith.

Correspondence between predicted and observed mass-relations among intermediate and more granitic rocks is more favorable. The present erosional level through the batholith intersects the solidified remnants of the MPOD and LQD fractionation chambers. Gradational zoning in both plutons (Fig. 2) ranges from quartz diorite margins to granodiorite cores. More granitic rocks invade their interiors. Fractionation must have proceeded by inward crystallization. Exposed volumes of these rocks (Table 5, Col. 3) compare favorably with the amounts expected. Cumulates formed by the computer model (Table 6) resemble the rocks in the margins of these plutons, and some hornblende

inclusions found in these rocks.

In conclusion, any single erosional level through a batholith will rarely permit observation of the entire spectrum of rocks and ^{of} volumes produced by fractional crystallization. Mafic and ultramafic cumulates produced by deeper-level fractionation can be expected to remain at depth. Residual liquids produced at any stage of differentiation can be consumed by later fractionation. The relative volumes of magmas remaining in batholiths is ^{also} dependent upon their relative timing of ascent, degree and depth of fractionation, and the amounts of magma withdrawn during eruption.

5. Emplacement-fractionation model

The evolutionary model envisioned here is one of initial emplacement of a single batch of high-alumina basalt (TPG) at depths > 8 to 10 km, followed by crystal settling modified by inward crystallization producing gabbroic and some pyroxenite cumulate, and a residual liquid of HHD. Early separation of olivine (Fo 77), hypersthene (En 77), augite (Di 76), plagioclase (An 65-50) and opaques produced the dioritic residual magma, HHD. This magma moved upward, invading and stopping the crystalline walls of the parental magma chamber, leaving ^{most} ~~much~~ of the cumulate behind at depth, ^{and thereby} producing the observed field relations at the present erosional level. Eruption of TPG parental magma and younger residual liquids may have occurred, but the volcanic cap is now eroded. The early appearance of hornblende in the intrusive series indicates that during ^{the} late stage of crystallization of TPG, ^{the} water content approached 2-4 wt.% in these liquids (43).

MPOD and LQD magmas rose closer to the surface < 8 to 10 km, and differentiated by inward crystallization, thereby progressively concentrating granitic components toward their cores. The youngest residual liquids were emplaced as dikes in the walls of their ^{parental} magma chambers.

^

In this manner, successive episodes of differentiation, followed by upward intrusion of progressively more granitic magmas, would account for the intrusive sequence and the rock associations observed in the batholith. Large amounts of mafic cumulate apparently remained behind in what were vertically-zoned differentiation chambers.

CONCLUSIONS

The Mount Stuart batholithic suite appears to represent the plutonic counterpart of the high-alumina basalt association. Computer modeling of the proposed fractionation process and all the available petrologic and field relationships indicate that the Mount Stuart suite is consanguineous, and that all phases of the suite can be derived from the oldest intrusive phase. Volume relations indicate that mafic cumulates formed at early stages of fractionation must lie at depth.

REFERENCES

1. Pratt, R.M.: The geology of the Mount Stuart area, Washington. Unpublished Ph.D. dissertation, Univ. Washington, 219p.(1953)
2. Russell, I.C.: A preliminary paper on the geology of the Cascade Mountains. U.S. Geol. Survey 20th Ann. Rpt. Pt. 2, 83-210 (1900)
3. Smith, G.O.: Description of the Mount Stuart Quadrangle. U.S. Geol. Survey Atlas, 106, Mount Stuart Folio, 10p.(1904)
4. Huntting, M.T., Bennett, W.G., Livingston, Jr., V.E., Moen, W.S.: Geologic map of Washington. Washington State Div. Mines Geol., Olympia 1961
5. Misch, P.: Tectonic evolution of the northern Cascades of Washington State - a west Cordilleran case history. In: Can. Inst. Min. Metal. Spec. Vol. 8, 101-148 (1966)
6. Page, B.M.: Geology of part of the Chiwaukum Quadrangle, Washington. Unpublished Ph.D. dissertation, Stanford Univ., 203p.(1939)
7. Plummer, C.C.: Geology of the crystalline rocks, Chiwaukum Mtns., and vicinity, Washington Cascades. Unpublished Ph.D. dissertation, Univ. Washington, 137p.(1969)
8. Frost, B.R.: Contact metamorphism of serpentinite, chlorite blackwall and rodingite at Paddy-Go-Easy Pass, central Cascades, Washington. J. Petrol. 16, 272-313 (1975)
9. Southwick, D.L.: Geology of the Alpine-type ultramafic complex near Mt. Stuart, Washington. Geol. Soc. Am. Bull. 85, 391-402 (1974)
10. Vance, J.A.: Geology of the Sauk River area, north Cascades. Unpublished Ph.D. dissertation, Univ. Washington (1957)
11. Yeats, R.S.: Geology of the Skykomish area in the Cascade Mountains of Washington. Unpublished Ph.D. dissertation, Univ. Washington, 243p.(1953)
12. Willis, C.L.: The Chiwaukum graben, a major structure of central Washington. Am. J. Sci. 251, 789-797 (1953)
13. Shapiro, L.: Rapid analysis of rocks and minerals by a single solution method. U.S. Geol. Survey Prof. Paper 557E, 187-191E (1967)
14. Medlin, J.H., Suhr, N.H., Bodkin, J.E.: Atomic absorption analysis of silicates employing LiBO₂ fusion. Atomic Abs. Newsletter 3, 25-29 (1969)
15. Mutschler, F.E., Rougon, D.R., Lavin, O.P.: PETROS, a data bank of major element chemical analyses of igneous rocks for research and teaching. Computers Geosci. in press(1976)
16. Flanagan, F.J.: U.S. Geological Survey silicate rock standards. Geochim. Cosmochim. Acta 31, 239-303 (1967)

17. Chayes, F.: Petrographic modal analysis. 113 p. New York: John Wiley 1956
18. Pongsapich, W.: Geology of the eastern part of the Mt. Stuart batholith, central Cascades, Washington. Unpublished Ph.D. dissertation, Univ. Washington, 170p.(1974)
19. Engels, J.C., Crowder, D.F.: Late Cretaceous fission-track and potassium argon ages of the Mount Stuart granodiorite and Beckler Peak stock, North Cascades, Washington. U.S. Geol. Survey Prof. Paper 750D, 39-43D (1972)
20. Erikson, E.H., Williams, A.: Implications of apatite fission track ages in the Mount Stuart batholith, Cascade Mountains, Washington (abst). Geol. Soc. Am. Programs, Cordilleran Sec. Mtgs. 3, p. 372 (1976)
21. Yeats, R.S., McLaughlin, W.A.: Radiometric age of three Cascade plutons, Skykomish area, Washington (abst). Geol. Soc. Am. Program Ann. Mtg., Mexico City, p.332 (1968)
22. Yeats, R.S., Engels, J.C.: Potassium-argon ages of plutons in the Skykomish-Stillaguamish areas, North Cascades, Washington. U.S. Geol. Survey Prof. Paper 750-D, 34-38D (1972)
23. Erikson, E.H.: Degranitization of the Late Cretaceous Mount Stuart batholith, central Cascades, Washington (abst). Geol. Soc. Am. Abs. Programs 5, p.39 (1973)
24. Holdaway, M.J.: Stability of andalusite and the aluminum silicate phase diagram. Am. J. Sci. 271, 97-131 (1971)
25. Richardson, S.W.: Staurolite stability in a part of the system Fe-Al-Si-O-H. J. Petrol. 9, 467-439 (1968)
26. Althaus, E., Karothe, E., Nitsch, K.H., Winkler, H.G.F.: An experimental re-examination of the upper stability limit of muscovite plus quartz. Neues Jahrb. Mineral, 7, 289-336 (1970)
27. Irvine, T.N., Baragar, W.R.A.: A guide to the chemical classification of the common volcanic rocks. Can. J. Earth Sci. 8, 523-548 (1971)
28. Bateman, P.C., Clark, L.D., Huber, N.K., Moore, J.G., Rinehart, C.D.: The Sierra Nevada batholith, a recent synthesis across the central part. U.S. Geol. Survey Prof. Paper 414D, 46p.(1963)
29. Erikson, E.H.: Petrology of the composite Snoqualmie batholith, central Cascades, Washington. Geol. Soc. Am. Bull. 80, 2213-2236 (1969)
30. Larsen, E.S.: Batholith and associated rocks of Corona, Elsinore, and San Luis Rey Quadrangles, southern California. Geol. Soc. Am. Mem. 29, 132p.(1948)
31. Nockolds, S.R., Allen, R.: The geochemistry of some igneous rock series. Geochim. Cosmochim. Acta, 4, 105-142 (1953)
32. Bowen, N.L.: The evolution of igneous rocks. 332 p. New York: Dover 1956

33. Kuno, H.: Origin of Cenozoic petrographic provinces of Japan and surrounding areas. *Volc. Bull.* 20, Ser. 2, 37-76 (1959)
34. Kuno, H.: High alumina basalt. *J. Petrol.* 1, 121-145 (1960)
35. Higgins, M.W.: Petrology of Newberry Volcano, Oregon. *Geol. Soc. Am. Bull.* 84, 445-488 (1973)
36. Smith, A.C., Carmichael, I.S.E.: Quaternary lavas from the southern Cascades, western USA. *Contrib. Mineral. Petrol.* 19, 212-233 (1968)
37. Waters, A.C.: Basalt magma types and their tectonic associations: Pacific Northwest of the United States. *In*, Crust of the Pacific Basin, *Am. Geophys. Union Mon.* 6, 158-170 (1962)
38. Wright, T.L., Deherty, P.C.: A linear-programming and least squares computer method for solving petrologic mixing problems. *Geol. Soc. Am. Bull.* 81, 1925-2207 (1970)
39. Deer, W.A., Howie, R.A., Zussman, J.: An introduction to the rock-forming minerals. 528 p. New York: John Wiley 1966
40. Dodge, F.C.W., Papike, J.J., Mays, R.E.: Biotites from granitic rocks of the central Sierra Nevada batholith, California. *J. Petrol.* 10, 250-271 (1969)
41. Larsen, E.S., Draisin, W.M.: Composition of the minerals in the rocks of the southern California batholith. *Rpt. 18th Geol. Cong., Great Britain, Pt. 2*, 66-79 (1950)
42. Orville, P.M.: Alkali ion exchange between vapor and feldspar phases. *Am. J. Sci.* 261, 201-237 (1963)
43. Holloway, J.R., Burnham, C.W.: Melting relations of basalt with equilibrium water pressure less than total pressure. *J. Petrol.* 13, 1-29 (1972)

EXPLANATION


QUATERNARY

 SURFICIAL DEPOSITS

EOCENE

 TEANAWAY BASALT DIKES

PALEOCENE

 SWAUK FORMATION


LATE CRETACEOUS


INTRUSIVE PHASES OF THE MT STUART BATHOLITH


 Microdiorite, diorite porphyry Tertiary?

 Aplite, granite, granite pegmatite

 Biotite trondhjemite

 Biotite hornblende granodiorite
 Biotite granodiorite


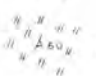
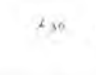

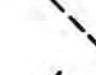

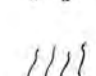
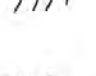

 Leucoquartz diorite
 Quartz diorite

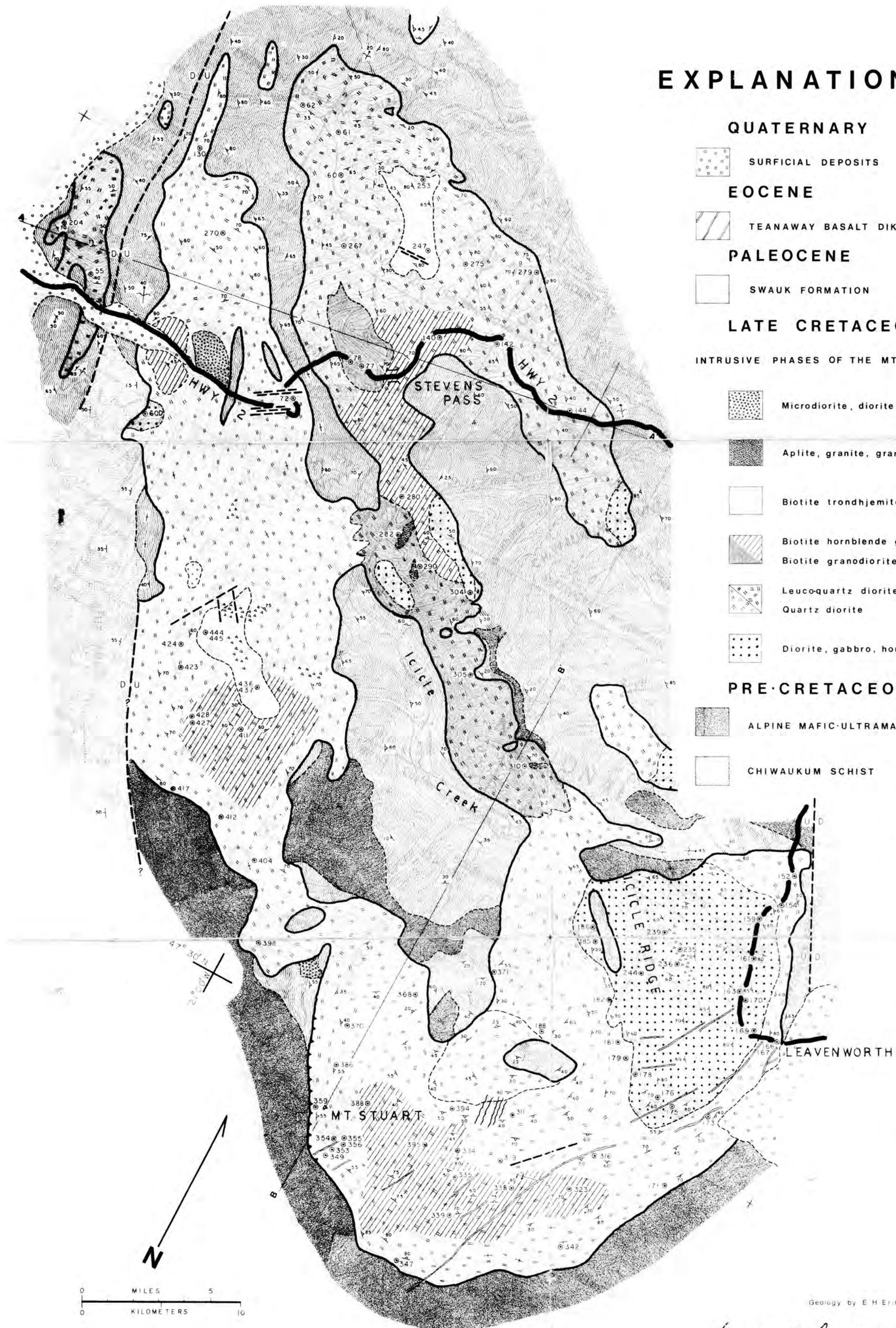
 Diorite, gabbro, hornblendite

PRE-CRETACEOUS

 ALPINE MAFIC-ULTRAMAFIC COMPLEX Jurassic?

 CHIWAUKUM SCHIST Paleozoic?

-  contacts
-  strike and dip of foliation
-  strike and dip of bedding
-  plunge of fold axes
-  faults
-  upper plate of thrust
-  cognate inclusion swarm
-  pegmatite dike swarm
-  analyzed sample



Geology by E. H. Erikson 1971, 1972, 1973

The Mount Stuart batholith and vicinity May, 1976
 ERIK H. ERIKSON

Explanation

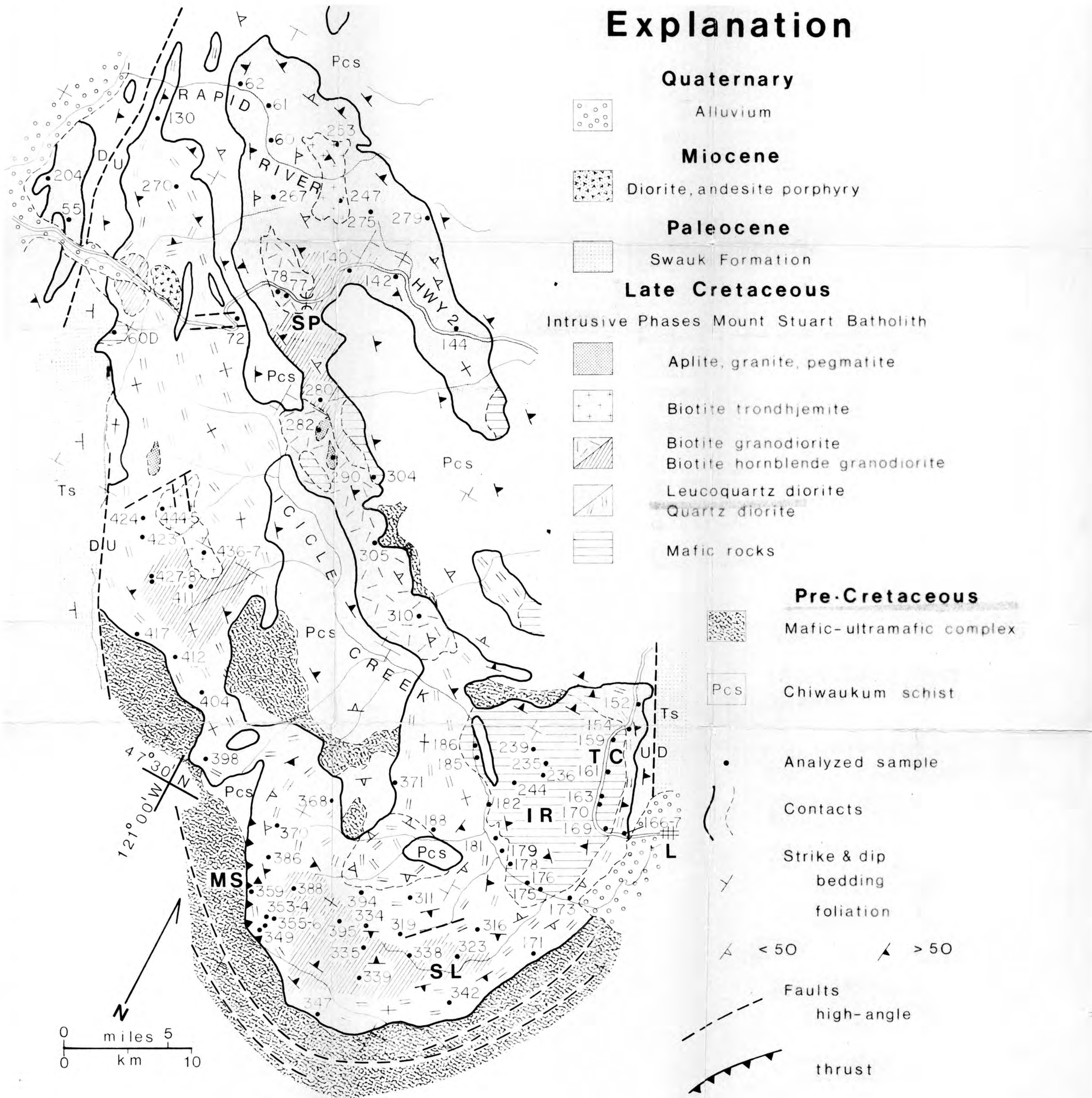


Fig 2. The Mount Stuart batholith and vicinity - from manuscript (June 1 1976)
 "Petrogenesis of the Mt. Stuart batholith"
 ERIC H. FRIKSON